Three-dimensional Nonlinear Plasmonic Metamaterials

Timo Stolt[a], Jeonghyun Kim[b], Sébastien Héron[c], Anna Vesala[a], Mikko J. Huttunen[a], Robert Czaplicki[d], Xiaorun Zang[e], Martti Kauranen[a], Junsuk Rho[b], and Patrice Genevet[c]

[a]Photonics Laboratory, Physics Unit, Tampere University, P.O. Box 692, FI-33101 Tampere, Finland
[b] Department of Mechanical Engineering, Pohang University of Science and Technology (POSTECH), Pohang 37673, Republic of Korea
[c]Université Côte d'Azur, CNRS - Centre de Recherche sur l'Hétéro-épitaxie et ses Applications, Valbonne, France
[d]Institute of Physics, Nicolaus Copernicus University, ul. Grudziadzka 5/7, 87-100 Toruń, Poland
[e]Faculty of Science and Forestry, Department of Physics and Mathematics, University of Eastern Finland,FI-80101 Joensuu, Finland

ABSTRACT

Three-dimensional (3D) metamaterials show the potential for realizing efficient nonlinear nanoscale devices. Despite the recent progress, the nonlinear metamaterials lack in terms of conversion efficiencies when compared against conventional nonlinear materials that rely on phase-matching techniques. Here, we demonstrate how the nonlinear responses of 3D metamaterials can be improved by stacking metasurfaces on top of each other and by applying phase-matching techniques. We demonstrate this by successfully fabricating phase-matched metamaterials consisting of stacked metasurfaces. Especially, we observe a 25-fold enhancement of second-harmonic generation emission from a device consisting of five metasurfaces.

Keywords: Nonlinear optics, metamaterials, plasmonics, phase-engineering

1. INTRODUCTION

Metamaterials and metasurfaces are artificial structures that consist of sub-wavelength building blocks called meta-atoms. With proper design of meta-atoms, metamaterials exhibit properties not found in natural materials, including magnetism at optical frequencies, strong optical activity, negative index of refraction, and epsilon-near-zero behavior.[1–4] Recently, phase-engineered metasurfaces have shown potential for the development of flat optical components, such as metalenses and polarizing interfaces.[5–7]

In addition to their linear optical properties, the nonlinear properties of metamaterials are a subject of growing interest. Numerous photonic technologies utilize nonlinear optical phenomena, such as second-harmonic generation (SHG), photon-pair generation, all-optical switching, frequency combs, and supercontinuum generation.[8–11] Unfortunately, the intrinsic nonlinear responses of materials are extremely weak. The traditional nonlinear materials compensate for this limitation with phase-matching schemes, which enables the nonlinear response to accumulate along the propagation in the material.[12] These relatively long propagation lengths are a significant limitation miniaturization of nonlinear optical devices, motivating the search for alternative enhancement methods.

Recently, plasmonic metamaterials, consisting of metal nanoparticles, have shown promise for realizing efficient nonlinear metamaterials.[13] The optical properties of metal nanoparticles are governed by the collective oscillations of the conduction electrons, known as localized surface plasmons. In resonance conditions, electromagnetic interactions between the incident field and plasmons give rise to localized surface plasmon resonances

Further author information: (Send correspondence to T.S.)
T.S.: E-mail: timo.stolt@tuni.fi, Telephone: +358 50 3740294

(LSPRs). This leads to a significant enhancement in local field near the particles.[14] As the nonlinear processes scale to the higher power of the local fields, the plasmon-driven field enhancements can result in dramatic enhances in the nonlinear responses of plasmonic materials. As a result, numerous investigations have studied the nonlinear optical properties of plasmonic metamaterials during the past decade.[15–19]

Here, we demonstrate a significant improvement in the nonlinear response of plasmonic metamaterials by utilizing phase-engineering principles. We fabricate metamaterial devices consisting of periodically stacked metasurfaces. With proper design of metasurface resonances and with proper selection of the stacking period, the devices become phase-matched to emit back-propagating SHG. The fulfilled phase-matching is confirmed with the measured SHG signal that increases monotonically with the number of layers.

2. THEORETICAL BACKGROUND

The conventional nonlinear materials achieve their strong nonlinear responses with accumulation of the signal over long enough propagation lengths. This requires that the both energy and momentum are conserved in the nonlinear process. The momentum conservation condition is also known as *phase-matching condition*, which for forward-propagating SHG is written as $\Delta k = 2k_\omega - k_{2\omega} = 0$, where $k_\omega = n_\omega \omega/c$ and $k_{2\omega} = n_{2\omega} 2\omega/c$ are the wavevector amplitudes at the fundamental (ω) and SHG (2ω) frequencies, respectively.[12] Traditionally, the phase-matching condition is fulfilled by taking advantage of birefringent crystals ($n_\omega = n_{2\omega}$) or by utilizing quasi-phase-matching techniques.[12,20,21]

Here, we design a phase-matched plasmonic metamaterial device that utilizes phase changes arising from the scattering of light from the nanoparticles. We use notations δ_ω and $\delta_{2\omega}$ for the phase changes at the fundamental and SHG frequencies, respectively. These terms are highly depended on the optical response of the nanoparticles, i.e. on their LSPRs.[7] Thus, by extending the phase-matching condition with δ_ω and $\delta_{2\omega}$, we can achieve phase matching with a proper metamaterial design. We demonstrate this capability by designing and fabricating metamaterial devices that were phase matched for back-propagating SHG (see Fig. 1). With conventional nonlinear materials, this type of phase-matching is difficult to realize, as it would require either negative refractive indexes or the use of complicated phase-matching schemes.

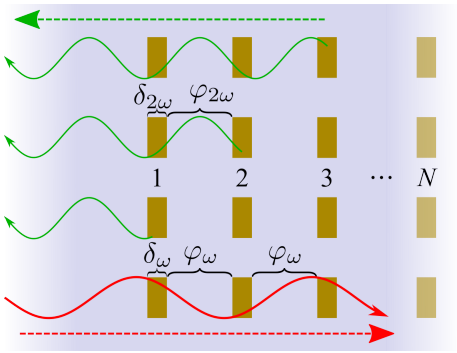

Figure 1. Schematic drawing of a metamaterial consisting of periodically stacked metasurfaces. The incident light and the generated SH signal are phase-shifted by the propagation between metasurfaces (φ_ω and $\varphi_{2\omega}$) and by the scattering from the nanoparticles (δ_ω and $\delta_{2\omega}$). With proper selection of the interlayer distances and with proper design of the metasurfaces, the metamaterial becomes phase matched for back-propagating SHG.

Our devices consisted of up to five ($N = 5$) stacked metasurfaces, surrounded by a homogeneous medium, and separated by distance h. To achieve phase matching, the accumulated phase of the back-propagating SHG signal should be a multiple of 2π. Now, we can write the phase matching condition for our devices as

$$2(\varphi_\omega + \delta_\omega) + \varphi_{2\omega} + \delta_{2\omega} = 2\pi m\,, \tag{1}$$

where m is an integer and terms $\varphi_{2\omega} = k_{2\omega} h$ and $\varphi_\omega = k_\omega h$ arise from the propagation of fields. With numerically estimated phase terms δ_ω and $\delta_{2\omega}$, the Eq. (1) allows to solve for h. Here, we estimated the phase terms by using the rigorous coupled wave analysis.[22,23]

3. RESEARCH METHODS

For this work, we fabricated metamaterial devices consisting of N metasurfaces composed of V-shaped gold nanoparticles arranged into square lattices with a lattice constant of $p = 1000$ nm. We chose this lattice configuration as it has shown to strongly enhance SHG.[24] The nanoparticles had arm lengths of $L = 180$ nm (L180-N) and $L = 220$ nm (L220-N), and arm widths of $w = 100$ nm resulting in LSPRs centered near 1060 nm. Then, according to Eq. (1), the back-propagating SHG becomes phase-matched by choosing $h = 225$ nm. For both device sets, L180-N and L220-N, the phase-matching condition was fulfilled for SHG process were both input and SHG signal were linearly polarized along the symmetry axis of the nanoparticles (y-axis, see Fig. 2).

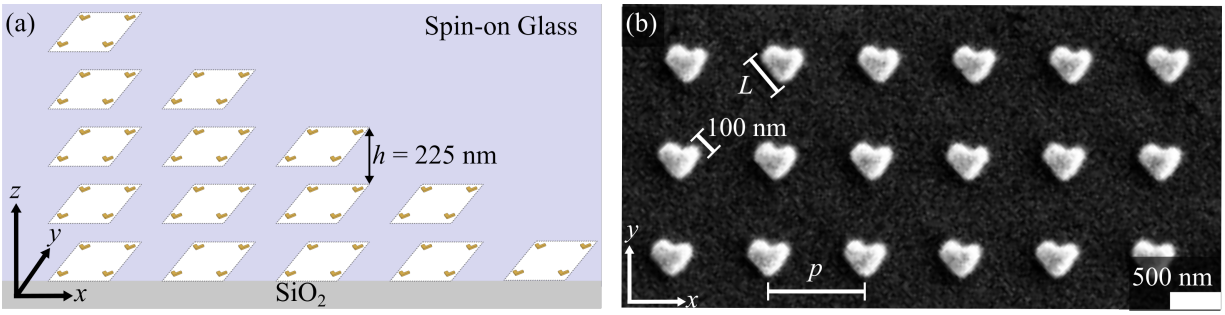

Figure 2. (a) The metasurfaces were stacked up to five layers ($N = 1$–5) on top of a silicon dioxide (SiO2) substrate. To fulfill the phase-matching conditions, each layer was separated by $h = 225$ nm.(b) Scanning electron micrograph from a metasurface consisting of V-shpaed gold nanoparticles. The nanoparticles had arm width of 100 nm and arm length of L. They were arranged into a square lattice with lattice period of $p = 1000$ nm giving rise to a LSPR around 1060 nm.

We fabricated the devices on fused silica (silicon dioxide SiO_2) substrate using a fabrication process consisting of following eight steps: i) spin-coating polymethyl methacrylate (PMMA) resist EL8 at 5000 rpm speed for one minute, and then baking the sample on a hot plate at 150°C for five minutes. ii) Spin-coating PMMA resist A2 at 2000 rpm for one minute and baking at 180°C for five minutes, iii) spin-coating a third layer of conductive polymer (E-spacer) at 2000 rpm for one minute, to avoid any charging effects during fabrication caused by the insulating substrate. iv) Electron beam lithography of the nanostructures and bathing in deionized water in order to remove the E-spacer. v) Development in methyl isobutyl ketone:isopropyl alcohol (1:3) solution for 12 minutes at 0°C followed by rinsing in isopropanol. vi) Deposition of a thin chromium layer (3 nm) and a layer of gold (20 nm) on the patterned resist by electron beam evaporation at 1 A/s. vii) Lift-off by bathing with acetone at 50°C for one minute. viii) Spin-coating spacer layer (spin-on-glass IC1-200) at 6000 rpm for one minute followed by baking at 250°C for five minutes in order to obtain a $h = 225$ nm thick spacer layer. In order to fabricate the complete device, this sequence was repeated then N times.

The SHG responses of the fabricated devices were characterized using the setup illustrated in Fig. 3. As a light source, we used an optical parametric oscillator (OPO) that was pumped with a pulsed Ti:sapphire laser with a center wavelength of 780 nm, pulse duration of 220 fs, and repetition rate of 80 MHz. In order to avoid possible sample damage, we limited the power of our light source to 10 mW. With a linear polarizer and a half-wave plate, we selected the correct polarization for the input laser beam. Then, the beam was focused on the sample that was aligned using a camera. The back-propagating SHG signal was guided with a dichroic mirror, metallic mirrors, and lenses to a photomultiplier tube (PMT) for photon detection. To ensure that only the light generated with OPO reached the sample and that only the SHG signal was measured, long- and short-pass filters were used along the beamline. By tuning the OPO wavelength from 1000 to 1300 nm, we measured the SHG emission spectra as function of the input wavelength.

4. RESULTS

The measured back-propagating SHG spectra are shown in Figs. 4(a) and 4(b) for the sets L220-N and L180-N, respectively. For the set L220-N, the signal increases with the increasing number of metasurfaces (N), but only up to $N = 2$. This might result from the fact that the phase-matching condition is not fulfilled, or that most of the incident light is absorbed after two metasurfaces. Fortunately, neither of these occur for the set L180-N.

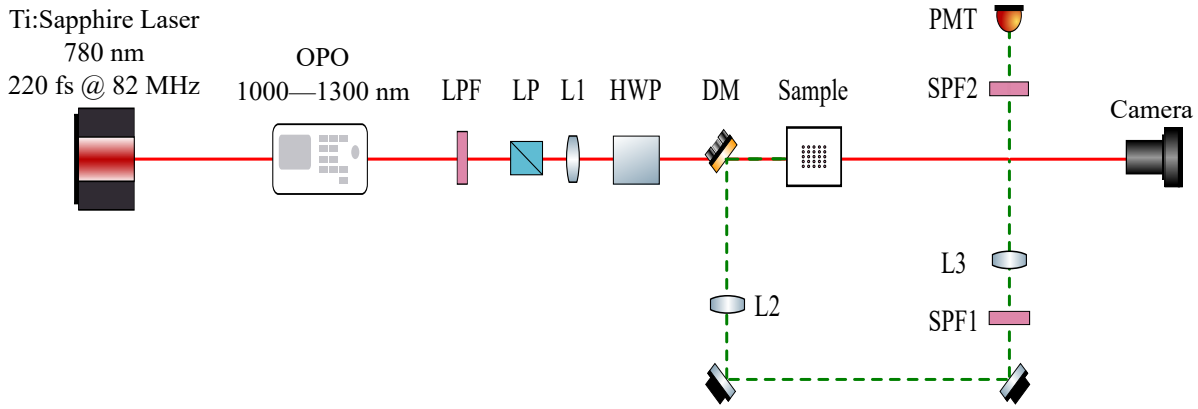

Figure 3. The experimental setup used to measure the back-propagating SH signal. An optical parametric oscillator (OPO) pumped with a Ti:sapphire femtosecond laser was used as a light source. The input power and polarization were controlled with a linear polarizer (LP) and a half-wave plate (HWP). The laser beam was weakly focused on a sample with a lens L1 and a camera was used to accurately aim the laser beam. The back-propagating signal was collected and guided to the photomultiplier tube (PMT) with dichroic mirror (DM) and lenses L2 and L3. The long-pass filter (LPF) assured that only the light generated with OPO reached the sample, while the short-pass filters (SPFs) assured that only the SH signal was measured.

Instead, the signal strength increases monotonically with N around the incident wavelength range 1100–1150 nm which we attribute as the region where the constructive phase matching occurs. The weakest signal is detected around 1000–1050 nm where the destructive phase matching occurs. The strongest SHG signal of 70 fW is emitted by the device L180-5 around the incident wavelength of 1120 nm. At this incident wavelength, the SH emission is no longer linearly dependent on N, but instead follows close-to quadratic dependence. This quadratic dependence further confirms the fulfilled phase matching. In addition, the devices were successfully phase matched in the challenging backward direction.[25]

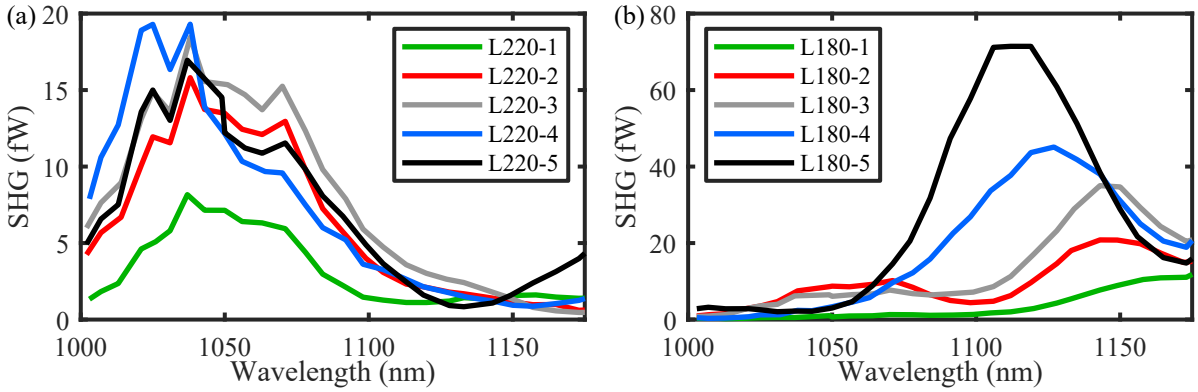

Figure 4. Measured SHG emission spectra for two set of metamaterials (a) L220-N and (b) L180-N. For L220-N, the phase-matching condition is not fulfilled and the SH emission does not improve by stacking more than two metasurface layers. For L180-N, the phase-matching condition is fulfilled and the SH emission increases monotonically with the number of layers.

In addition to the successful phase matching, another interesting feature is detected from L180-N emission spectra. The emission peaks blueshift from 1150 nm to 1120 nm when N increases from three to five (see Fig. 4(b). This behaviour could result from the optical coupling of adjacent metasurfaces.[26,27] It has been shown with planar metasurfaces, that the optical coupling of adjacent nanoparticles can result in collective responses known as surface lattice resonances, that enhance the SHG emissions from metasurfaces.[24,28–30] It seems plausible that similar effects could occur also along the propagation direction.[27] Unfortunately, due to the difficulties in our novel fabrication process, we could not yet fully control the relative position of adjacent metasurfaces. In the

future, however, we aim to overcome this lack of control and properly design the optical coupling between the metasurfaces. Then, the combined impact of phase matching and optical coupling could pave the way towards efficient nonlinear metamaterials.

5. CONCLUSION

To conclude, we demonstrated how to improve the nonlinear responses of metamaterials by stacking metasurfaces into three-dimensional devices. These devices can be easily phase-matched by controlling the nanoparticle dimension and the separation between the adjacent metasurfaces. We confirmed this ability by phase-matching back-propagating second-harmonic generation, which is a difficult task to fulfill using conventional nonlinear materials. We fabricated metamaterial devices consisting of up to five stacked metasurfaces and demonstrated a clear monotonic increase in the second-harmonic signal with the increasing number of metasurfaces. Our results show promise for further development of three-dimensional metamaterials, that could utilized for example to realize more efficient nonlinear metamaterials.

ACKNOWLEDGMENTS

The authors wish to thank all the collaborators at Tampere University, Pohang University of Science and Technology, Université Côte d'Azur, Nicolaus Copernicus University, and University of Eastern Finland for they work and input. We also wish to thank Photonics Research and Innovation (PREIN) flagship for funding our research.

REFERENCES

[1] Soukoulis, C. M. and Wegener, M., "Past achievements and future challenges in the development of three-dimensional photonic metamaterials," *Nature Photonics* **5**, 523 (jul 2011).

[2] Linden, S., Enkrich, C., Dolling, G., Klein, M. W., Zhou, J., Koschny, T., Soukoulis, C. M., Burger, S., Schmidt, F., and Wegener, M., "Photonic metamaterials: Magnetism at optical frequencies," *IEEE Journal on Selected Topics in Quantum Electronics* **12**(6), 1097–1104 (2006).

[3] Alù, A., Silveirinha, M. G., Salandrino, A., and Engheta, N., "Epsilon-near-zero metamaterials and electromagnetic sources : Tailoring the radiation phase pattern," *Physical Review B* **75**, 155410 (2007).

[4] Zhang, S., Park, Y.-S., Li, J., Lu, X., Zhan, W., and Zhang, X., "Negative index in chiral metamaterials," *Physical Review Letters* **102**, 023901 (2009).

[5] Yu, N. and Capasso, F., "Flat optics with designer metasurfaces," *Nature Materials* **13**(2), 139–150 (2014).

[6] Yin, X., Steinle, T., Huang, L., Taubner, T., Wuttig, M., Zentgraf, T., and Giessen, H., "Beam switching and bifocal zoom lensing using active plasmonic metasurfaces," *Light: Science & Applications* **6**(7), e17016 (2017).

[7] Genevet, P., Capasso, F., Aieta, F., Khorasaninejad, M., and Devlin, R., "Recent advances in planar optics: from plasmonic to dielectric metasurfaces," *Optica* **4**(1), 139 (2017).

[8] Kwiat, Paul G and Mattle, Klaus and Weinfurter, Harald and Zeilinger, Anton and Sergienko, Alexander V and Shih, Y., "New high-intensity source of polarization-entangled photon pairs," *Physical Review Letters* **75**(24), 4337 (1995).

[9] Brabec, T. and Krausz, F., "Intense few-cycle laser fields: Frontiers of nonlinear optics," *Reviews of Modern Physics* **72**(2), 545 (2000).

[10] Kippenberg, T. J., Holzwarth, R., and Diddams, S. A., "Microresonator-Based Optical Frequency Combs," *Science* **332**(April), 555–560 (2011).

[11] Shcherbakov, M. R., Vabishchevich, P. P., Shorokhov, A. S., Chong, K. E., Choi, D. Y., Staude, I., Miroshnichenko, A. E., Neshev, D. N., Fedyanin, A. A., and Kivshar, Y. S., "Ultrafast All-Optical Switching with Magnetic Resonances in Nonlinear Dielectric Nanostructures," *Nano Letters* **15**(10), 6985–6990 (2015).

[12] Boyd, R. W., [*Nonlinear optics*], Academic Press, San Diego (2003).

[13] Kauranen, M. and Zayats, A. V., "Nonlinear plasmonics," *Nature Photonics* **6**, 737–748 (2012).

[14] Maier, S. A., [*Plasmonics: Fundamentals and applications*] (2007).

[15] Lapine, M., Shadrivov, I. V., and Kivshar, Y. S., "Colloquium: Nonlinear metamaterials," *Reviews of Modern Physics* **86**(3), 1093–1123 (2014).

[16] Butet, J., Brevet, P. F., and Martin, O. J., "Optical Second Harmonic Generation in Plasmonic Nanostructures: From Fundamental Principles to Advanced Applications," *Acs Nano* **9**(11), 10545–10562 (2015).

[17] Li, G., Zhang, S., and Zentgraf, T., "Nonlinear photonic metasurfaces," *Nature Reviews Materials* **2**(5) (2017).

[18] Rahimi, E. and Gordon, R., "Nonlinear Plasmonic Metasurfaces," *Advanced Optical Materials* **6**(18), 1–9 (2018).

[19] Huttunen, M. J., Czaplicki, R., and Kauranen, M., "Nonlinear plasmonic metasurfaces," *J. Nonlinear Opt. Phys. Mater.* **28**, 1950001 (mar 2019).

[20] Pelton, M., Marsden, P., Ljunggren, D., Tengner, M., Karlsson, A., Fragemann, A., Canalias, C., and Laurell, F., "Bright, single-spatial-mode source of frequency non-degenerate, polarization-entangled photon pairs using periodically poled KTP," *Optics Express* **12**, 3573 (jul 2004).

[21] Hu, X. P., Xu, P., and Zhu, S. N., "Engineered quasi-phase-matching for laser techniques [Invited]," *Photonics Research* **1**, 171 (dec 2013).

[22] Glytsis, E. N. and Gaylord, T. K., "Rigorous three-dimensional coupled-wave diffraction analysis of single and cascaded anisotropic gratings," *Journal of the Optical Society of America A* **4**(11), 2061 (1987).

[23] Lalanne, P. and Silberstein, E., "Fourier-modal methods applied to waveguide computational problems," *Optics Letters* **25**, 1092 (aug 2000).

[24] Czaplicki, R., Kiviniemi, A., Huttunen, M. J., Zang, X., Stolt, T., Vartiainen, I., Butet, J., Kuittinen, M., Martin, O. J. F., and Kauranen, M., "Less is more – enhancement of second-harmonic generation from metasurfaces by reduced nanoparticle density," *Nano Letters* **18**(12), 7709–7714 (2018).

[25] Liu, L., Wu, L., Zhang, J., Li, Z., Zhang, B., and Luo, Y., "Backward Phase Matching for Second Harmonic Generation in Negative-Index Conformal Surface Plasmonic Metamaterials," *Adv. Sci.* **5**(11), 1–8 (2018).

[26] Huttunen, M. J., Dolgaleva, K., Törmä, P., and Boyd, R. W., "Ultra-strong polarization dependence of surface lattice resonances with out-of-plane plasmon oscillations," *Optics Express* **24**(25), 28279 (2016).

[27] Segal, N., Keren-Zur, S., Hendler, N., and Ellenbogen, T., "Controlling light with metamaterial-based nonlinear photonic crystals," *Nature Photonics* **9**, 180–184 (mar 2015).

[28] Michaeli, L., Keren-Zur, S., Avayu, O., Suchowski, H., and Ellenbogen, T., "Nonlinear Surface Lattice Resonance in Plasmonic Nanoparticle Arrays," *Physical Review Letters* **118**(24), 970 (2017).

[29] Huttunen, M. J., Rasekh, P., Boyd, R. W., and Dolgaleva, K., "Using surface lattice resonances to engineer nonlinear optical processes in metal nanoparticle arrays," *Physical Review A* **97**, 053817 (2018).

[30] Hooper, D. C., Kuppe, C., Wang, D., Wang, W., Guan, J., Odom, T. W., and Valev, V. K., "Second harmonic spectroscopy of surface lattice resonances," *Nano Letters* , acs.nanolett.8b03574 (2018).